Hindawi
Geofluids
Volume 2020, Article ID 6617468, 26 pages
https://doi.org/10.1155/2020/6617468

Research Article

Ground Settlement of High-Permeability Sand Layer Induced by Shield Tunneling: A Case Study under the Guidance of DBN

Cong Zhou, Wei Gao, Shuang Cui, Xiaochun Zhong, Chengjie Hu, and Xin Chen

Key Laboratory of Ministry of Education for Geomechanics and Embankment Engineering, College of Civil and Transportation Engineering, Hohai University, Nanjing 210024, China

Correspondence should be addressed to Wei Gao; wgaowh@163.com

Received 20 October 2020; Revised 6 November 2020; Accepted 11 November 2020; Published 21 November 2020

Academic Editor: Bin Gong

During the shield construction of Harbin Subway Line No. 3 Project, the average ground settlement exceeds the warning value. In order to find the cause of settlement and improve it, this paper establishes a settlement prediction model to analyse the potential influencing factors based on the Deep Belief Network (DBN) and calculated the correlation degree between influencing factors and settlement through sensitivity analysis. It was found that the permeability coefficients of layer and cutter head torque are the main factors affecting settlement. Then, corresponding muck improvement measures were made according to the analysis of the layer conditions, which successfully reduced the permeability and shear strength of the muck, thereby controlling the surface settlement value within the warning range. The research results in this paper illustrate the applicability and robustness of DBN in tunnel engineering, and the related research ideas can be applied to other projects.

1. Introduction

The surface settlement caused by the subway shield construction will have a greater impact on the surrounding buildings and underground pipelines. How to control the settlement within a reasonable range has been a hot spot in the research of shield construction. In the construction of the second phase of the Harbin Subway Line No. 3 Project, it was found that the average settlement value of one construction section exceeded the warning value when the right-line tunnel was excavated to the 150th ring, and the settlement values of some measuring points exceed the maximum allowable value. As the construction section of the tunnel is laid along the avenue, there are various pipelines above the construction tunnel, such as water supply pipelines, natural gas pipelines, and electric power pipelines. The minimum space between the pipelines and tunnel is only 2 m. Moreover, the surrounding buildings are residential areas and hospital, which are mostly frame structures and only about 30 m away from the tunnel axis. For the safety of underground pipelines, surrounding buildings, and ground transportation, it will be very urgent to find the cause of ground settlement and solve it in time.

Due to the variability of actual working conditions, theoretical research is limited; many scholars have conducted research on the ground settlement through laboratory experiments and numerical simulation. For example, based on the construction of Tabriz Subway Line 2, Sharghi et al. [1] studied the effect of the grout properties on the surface settlement. The results show that the amount of grouting has little effect on the settlement, but the grout with higher compressive strength can control the settlement. Xie et al. [2] took the Yingbin No. 3 Road Tunnel in Shanghai as an example, which showed that grouting pressure and quality influence the surface settlement by using a three-dimensional finite difference method. With the help of finite element software, Eskandari et al. [3] found that surface settlement is related to EPB (Earth Pressure Balance) pressure based on the example of Mashhad Metro. Kim et al. [4] built a 3-D hydromechanical coupled finite element model which simulates the entire process of shield tunneling to study the effect of shield

face pressure and backfill pressure on the tunneling-induced surface settlement and found that a moderate increase in the face pressure and backfill pressure can control surface settlement. In the study on the improvement of muck soil to control surface settlement, Cui and Lin [5] carried out the screening test and field test to determine the reasonable ratio of muck improver for shield tunneling in water-rich sandy cobble ground. Based on a special device to simulate soil tank and screw conveyor, Peila et al. [6] carried out the slump tests to analyse the impact of different foam mortar and the moisture content in the soil on the surface settlement. Fritz [7] carried out the suspension pressure and the corresponding penetration depth tests and found that adding sand, vermiculite and polymer additives to the mud can effectively meet the requirements of mud film formation and reduce the surface settlement. Through the direct shear test and pressure penetration test, Psomas [8] found that the application of soil improvement can reduce the surface settlement in earth pressure balanced shield construction. Based on the analysis of previous research, it is found that the laboratory tests are more direct for solving engineering problems, and the causes of ground settlement can be found through test measurements. However, there are multiple factors that induce ground settlement during shield construction. The laboratory tests or numerical simulations cannot consider all potential influencing factors, and their advantage is to conduct research on a specific influencing factor [9–12]. In order to find the main factors that affect settlement, a systematic analysis of potential influencing factors is required.

At present, with the advent of the big data era, many scholars have gone through deep learning to explore the factors of surface subsidence caused by shield construction [9–13]. Deep learning uses big data to learn features, which is more capable of portraying data-rich internal information [14]. It shown significant advantages in multifactor system analysis than traditional methods [9–12]. For example, Boubou et al. [15] used artificial neural networks to establish the relationship between the construction parameters of the shield and the ground settlement. With the development of deep learning methods, Chen et al. [16] used general regression neural network (GRNN) model to consider the nonlinear relationship between maximum ground surface settlements and geometry, geological conditions, and shield operation parameters. The results show that the predicted value of the GRNN model is close to the measured one. [9–12] used a back-propagation neural network (BPNN) to predict the tunneling-induced settlement, and the sensitivity analysis indicates the geological and geometric parameters are the most influential variables for the settlement. Bouayad and Emeriault [17] proposed a methodology that combines the Principal Component Analysis (PCA) with Adaptive Neuro-Fuzzy-based Inference System (ANFIS) to model the nonlinear relationship between ground surface settlements and the operational and geological parameters. Lyu et al. [18] proposed an improved trapezoidal fuzzy analytic hierarchy process (FAHP) to assess the risk of mega city infrastructures related to land subsidence in Shanghai and indicates that the trapezoidal FAHP method can be used to effectively capture the high risks for significant industrial infrastructures related to land subsidence. The above studies established the relationship between surface settlement and various construction parameters through deep learning, which is helpful to guide people to consider which factors should be considered in the study of surface settlement.

In response to the problem of excessive ground subsidence in the construction of Harbin Subway, this paper will adopt a currently applied deep learning method to analyse potential influencing factors of settlement, namely, Deep Belief Networks (DBN). In this paper, the authors will establish the relationship between potential influencing factors and surface settlement based on DBN, and use the grey relational analysis method to conduct a sensitive analysis of various influencing parameters, find the main factors, and improve them to control the surface settlement. Besides, the method of solving engineering problems based on the guidance of deep learning can be promoted in future tunnel construction.

2. Overview of Harbin Subway Project

2.1. Engineering Overview. The second part of the No. 3 Line of Harbin Subway is a circular line in the Harbin Subway network (Figure 1). The construction method between Qunli Sixth Avenue Station and Gongnong Avenue Station is shield tunneling. The start time is July 25, 2017. This section is laid along Lijiang Road, in which the tunnel length is 693.997 m, and the distance between the left and right lines is 14 m. Among them, the left line construction precedes the right line. The right line is designed with a mileage of CK41+619.450 to CK42+313.447. The section has a herringbone slope in the longitudinal direction, with a downhill slope of 5‰, an uphill slope of 11.64‰, a maximum soil cover of 10.38 m, and a minimum soil cover of 6.96 m. The buried depth of the tunnel roof is about 8.5 m, and the tunnel diameter is 6.2 m.

2.2. Geological Condition. According to the geological survey, the geomorphic units along this tunnel section belong to the flood plain and first-level terraces of the Songhua River. The ground elevation is between 130 and 138 m, the natural height difference is less than 8 m, and the terrain is relatively gentle.

The properties of each soil layer in this interval are summarised in Table 1. Figure 2 is the geological profile of the tunneling section. The main layers that the shield tunnel passed through are fine sand (layer 2-3) and medium-coarse sand (layer 2-4), and it partially crosses silty clay (layer 2-1). The upper part of the tunnel is plain-filled soil (layer 1-2), silty clay (layer 2-1), and fine sand (layer 2-3). The lower part of the tunnel is mainly medium-coarse sand (layer 2-4) and silty clay (layer 7-1).

In order to ascertain the groundwater connection and hydrogeological parameters in the site, a pumping test was set up at this site. The pumping test of the single-well nonintact well with secondary drawdown was used, and the hydrogeological parameters of the aquifer were calculated using steady flow. The calculation results of hydrogeological parameters for this pumping test are shown in Table 2. From Table 2, the stratum has poor stability and strong water permeability, which is prone to flow sand and water permeability. From the perspective of construction excavation, the shield construction area is mainly composed of coarse sand and fine

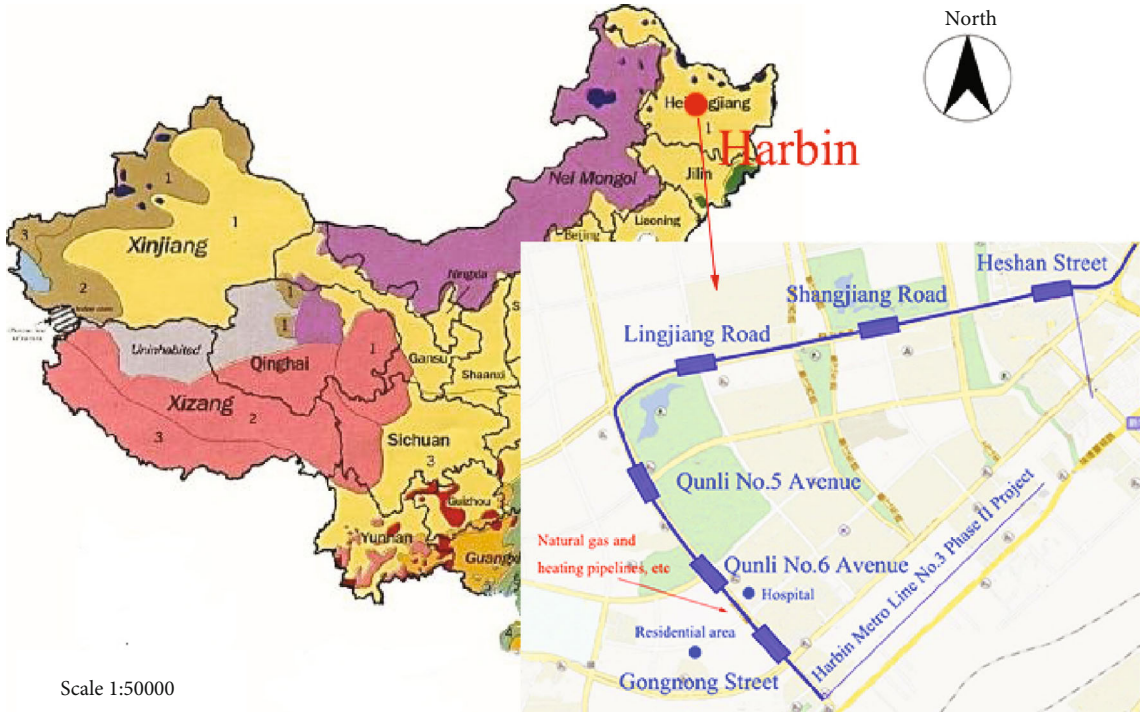

Figure 1: Subway project site.

Table 1: Physical properties of soil layers.

Soil layer number	Soil layer name	Natural moisture content w (%)	Natural density ρ (g/cm^3)	Void ratio e	Poisson's ratio ν	Cohesion c (kPa)	Internal friction angle φ (°)	Characteristic value of bearing capacity of foundation soil f_{ak} (kPa)	Permeability coefficient (cm^{-6}/s) Horizontal k_h	Vertical k_v
1-2	Plain fill	—	1.8	—	—	—	—	—	—	—
2-1	Silty clay	32.14	1.83	0.97	0.35	16.90	7.82	100	7.6	8.9
2-3	Fine sand	16.45	2.00	0.56	0.30	3.5	24.93	140	—	8246.2
2-4	Coarse sand	11.12	2.09	0.42	0.30	0	32.0	290	—	31925.0
2-4-1	Silty clay	29.66	1.92	0.83	0.35	38.56	12.00	135	15.6	8.4
7-1	Silty clay	28.88	1.95	0.80	—	37.38	12.45	—	—	—
7-2	Coarse sand	10.53	2.08	0.42	0.35	0	35.39	150	13.6	16.2
7-3	Silty clay	27.83	1.97	0.78	0.30	37.38	12.45	300	—	24000

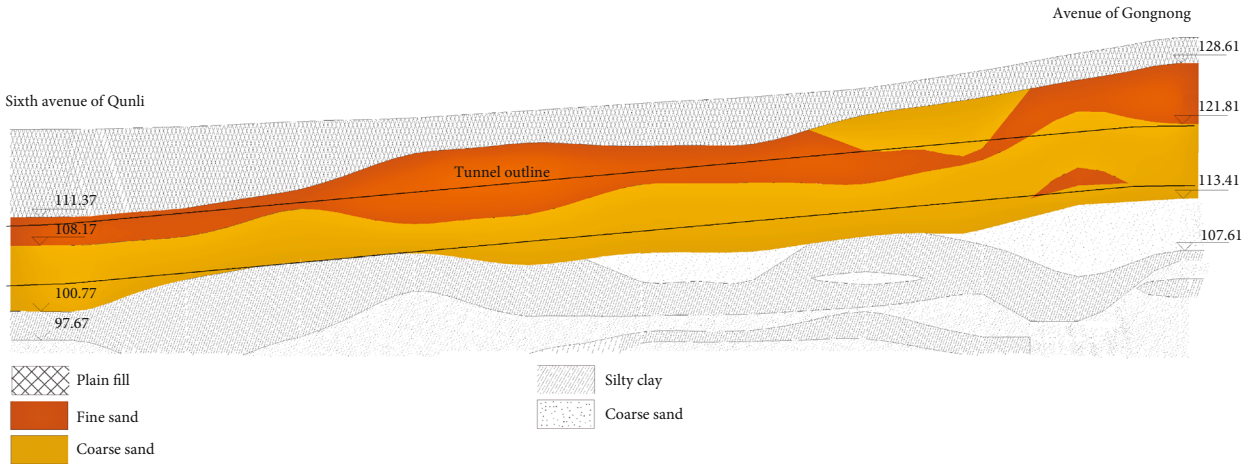

Figure 2: Geological profile.

Table 2: Parameters and results of pumping test.

	Pumping time (h)	Drawdown (m)	Pumping stability time (h)	Permeability coefficient (m/d)	Radius of influence (m)
First drawdown	20	2.71	8	25.50	214
Second drawdown	21	4.09	8	21.12	214
Average value	20.5	3.40	8	23.31	214

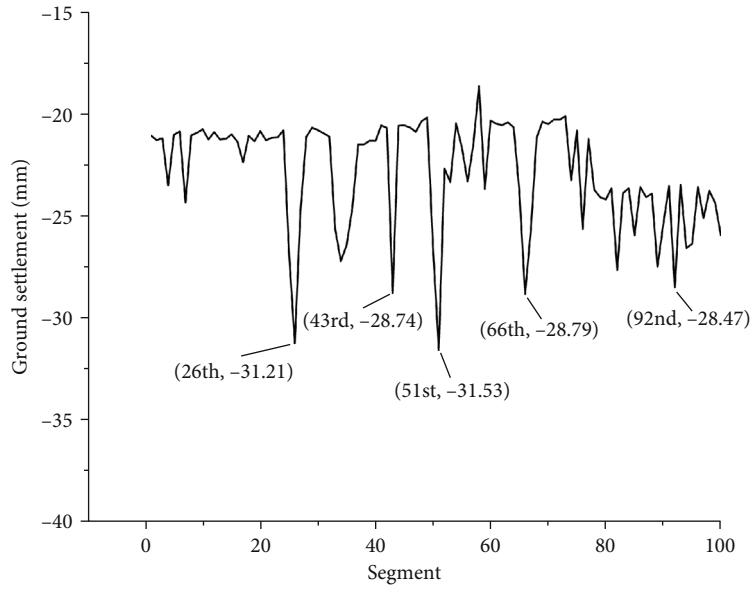

Figure 3: Settlement value of the first 100 rings on the right line.

sand in rich water. The medium-coarse sand layer contains saturated water, and the mud content is low. Thus, the muck has low viscosity and strong permeability, whose workability and fluidity are low.

2.3. Description of Settlement Problem. The right line of Qunli Sixth Avenue to Gongnong Avenue Station broke the gate on July 25, 2017; the completion time of the left line is August 16, 2017. In the initial stage of monitoring, there is no significant settlement occurred. However, with the advancement of the shield machine, the ground settlement has become more extensive. Figure 3 shows the ground settlement for each measuring point within 100 rings. At this time, the segment assembly is completed with 152nd ring, and the incision is located at 159th ring.

According to Figure 3, it can be seen that the settlement value of each measuring point of the first 100 rings reached -22.80 mm, which exceeded the settlement warning value (Table 3). Among them, the settlement value of some measuring points directly exceeds the maximum allowable value (30 mm). The number of segments corresponding to the points exceeding the maximum allowable value is 26th and 51st rings, and their settlement values are 32.21 mm and 32.53 mm, respectively, which exceed the warning value by 12.21 mm and 12.53 mm, respectively. Also, the settlement values of 34th, 35th, 43rd, 66th, and 82nd rings will also approach the maximum allowable value.

Table 3: Engineering control standards.

Monitoring project	Control value (mm)	Cumulative warning value		
		Yellow	Orange	Red
Ground settlement	-30 mm	-21 mm	-25.5 mm	-30 mm
(Bulge)	+10 mm	+7 mm	+8.5 mm	+10 mm
Segment uplifting	+20 mm	+10 mm	+15 mm	+20 mm

It can be known from Introduction in Section 1 that there are many essential pipelines above the shield segment, and the surrounding buildings are not far away. If the ground settlement cannot be well controlled, it will have a more significant impact on the pipelines and surrounding buildings. At the same time, it can be found that the assembly quality of the tunnel segments also has problems. There were misalignments in multiple segments, which were manifested as misalignment at the top of the segment and lateral misalignment of the segment. And several bottom segments were leaking and damaged (Figure 4). It may be caused by the uplifting of the segments and construction errors, and the specific influencing factors need to be further analysed below.

Considering the various potential hidden dangers caused by excessive ground settlement, it is necessary to analyse the

(a) (b) (c)

Figure 4: Map of segment assembly.

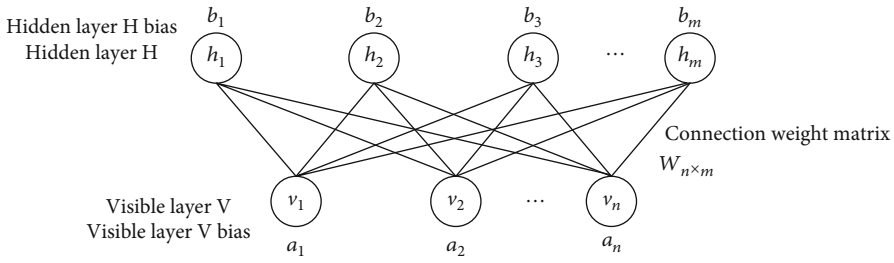

(a) RBM structure model of restricted Boltzmann machine

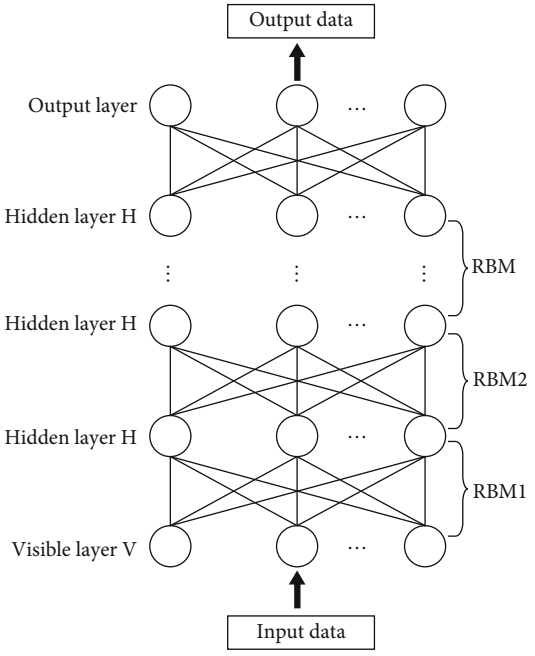

(b) DBN structure diagram

Figure 5: Diagram of Deep Belief Network (DBN).

factors that may induce subsidence one by one, find the problem, and solve it, so as to control the surface subsidence within a reasonable range.

3. Analysis of Factors Influencing Ground Settlement

3.1. Establishment of a Prediction Model Based on the Deep Belief Network. In order to accurately locate the most influential parameters, this paper proposes a prediction model based on the deep belief network to analyse the impact of each-construction parameter.

Deep Belief Network (DBN) is an artificial neural network in deep learning. Compared with traditional neural networks, DBN uses Restricted Boltzmann Machine (RBM) learning algorithms to enhance the ability of neural network data feature extraction and to enable neural network prediction which is greatly enhanced [19].

RBM is the basic module of DBN (Figure 5). An RBM model consists of two layers of neurons (the visible layer and the hidden layer). DBN is made up of multiple RBM structures stacked one after another [20]. The visible layer of the first RBM is used to receive input data, and the hidden layer of the first RBM is also the visible layer of the second RBM, and so on. One RBM hidden layer neuron is used as the visible layer neuron of the next RBM, stacked layer by layer to form a DBN model with multiple hidden layers (Figure 5).

In shield construction, the shield construction parameters, geological conditions, and grouting conditions are the main factors that cause surface settlement and the quality of segment assembly [21]. In this paper, eight factors including soil pressure, jack thrust, cutter head torque, tunneling speed, grouting volume, grouting pressure, layer permeability coefficient, and slurry density are selected as input layers, and the amount of surface settlement and uplifting segment volume are used as output layers to establish a DBN prediction model, to study the influence of various parameters on the settlement and segments. This paper selects a typical DBN model with 2 hidden layers. The number of input nodes is 8, which represents eight construction parameters. And the number of output nodes is 2, which indicates the predicted value of the ground settlement and the predicted value of segment uplifting. The model training process is divided into two steps: the first step is to pretrain the RBM, and the number of neurons, the learning rate, and other parameters need to be continuously adjusted and optimised during the training process. Finally, the number of neurons in the two hidden layers of RBM is determined to be 48 and 12, the learning rate is 0.00001, and the performance function MSE and the activation function Sigmoid are used. Due to the consistency of the geological conditions on the left and right lines, the training set of the model is based on the settlement data of the left line, and the 1-150 ring data of the right line is selected as the test set. The prediction results of the test set are shown in Figure 6.

From Figure 6, although there are a few points that have large deviations between the measured and predicted values of surface settlement and segment uplifting, but the overall effect is better. The mean square error of the surface settlement is 0.051, and the mean square error of the uplifting amount of the segments is 0.044; it can be seen that the accuracy of the model prediction is higher [22]. Because there are many accidental influence factors in actual construction, this article comprehensively considers the influence of construction parameters and geological conditions.

3.2. Analysis of Construction Parameters and Geological Conditions. Section 4.1 establishes a DBN prediction model for surface settlement and segment uplifting based on influencing factors such as soil pressure, jack thrust, cutter head torque, tunneling speed, grouting volume, grouting pressure, permeability coefficient, and slurry density. Through the analysis of the prediction model, it is possible to explore the relationship between each input and output during the shield construction process, which helps to reveal the influence of these shield tunneling parameters on the ground settlement.

In the study of the influence of soil pressure, this paper takes all the 658 rings data on the left line as the training set in which there are 16 sets of data. In this training set, the soil pressures are 1.5, 1.6, 1.7, 1.8,...,3, and the other tunneling parameters are the average values. Since the test set requires the input of surface settlement and uplifting segment data, according to the predicted value (Figure 6), here the surface subsidence is set to -20 and the segment uplifting is set to 3. The output result is shown in Figure 7(a). Similarly, the output results of the other tunneling parameters are shown in Figures 7(b)–7(h).

It can be seen from Figure 7 that as the pressure of the soil increases, the ground settlement value gradually decreases, but the uplifting value of the segment increases in a similar range. The greater the jack thrust, cutter head torque, and tunneling speed, the greater the surface settlement. However, the cutter head torque and tunneling speed have little effect on the segment, while the jack thrust has a noticeable impact on the segment. In addition, the influence of grouting volume and grouting pressure on the settlement is consistent, that is, the greater the grouting volume and grouting pressure, the smaller the ground settlement. Moreover, the larger the grouting amount is, the smaller the uplifting amount of the segments will be. However, the grouting amount cannot be increased unambiguously, and the higher the grouting amount means, the higher the construction cost. Moreover, the higher the grouting pressure is, the higher the floating amount of the segment will be. Finally, the permeability coefficient and the slurry density also have an essential influence on the surface settlement. The greater the permeability coefficient, the greater the surface settlement value, and the higher the slurry density, the smaller the surface settlement value. The influence of these two parameters on the segment is also apparent.

3.3. Sensitivity Analysis of Influencing Factors. In order to study the influence of the influencing factors deeply, the ground settlement will be taken as the representative indexes, and the correlations between the representative indexes and the influencing factors are calculated by the grey relational analysis method [23] to study the sensitivity of influencing factors.

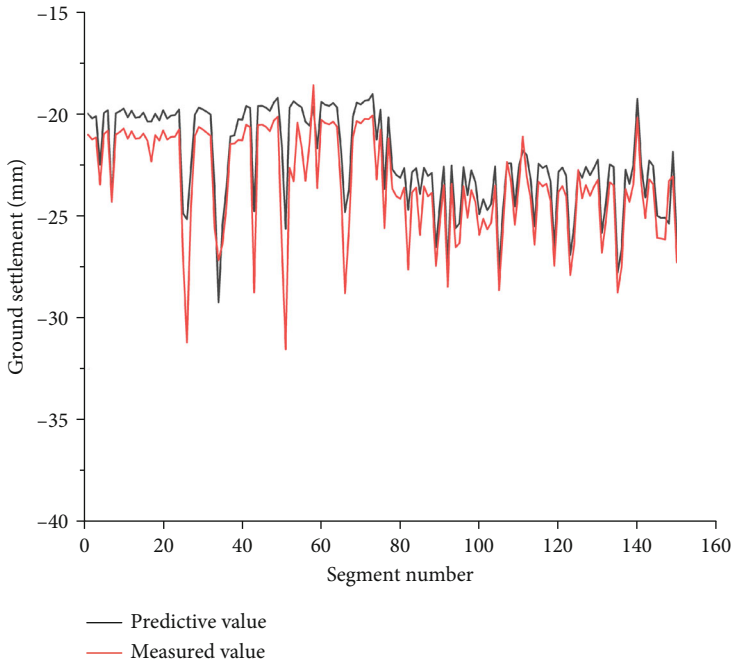

(a) Predicted output value of surface settlement

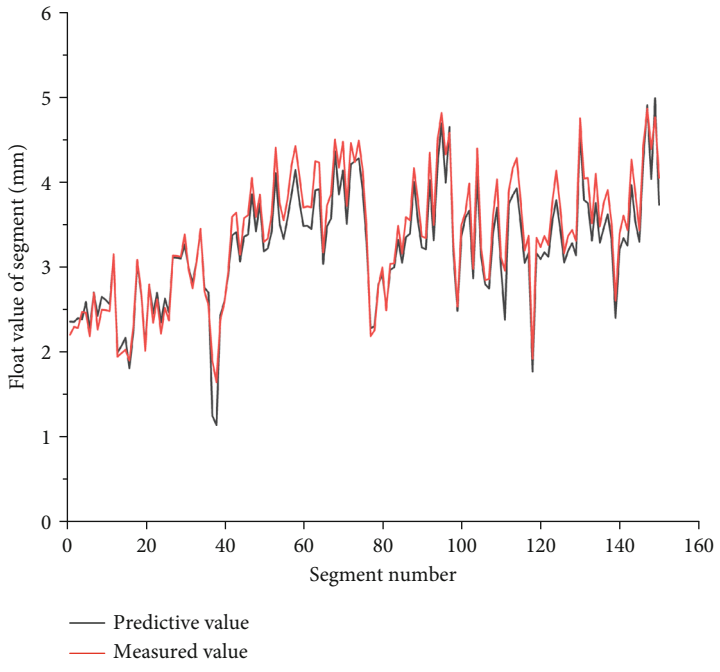

(b) Predicted output value of segment uplift

Figure 6: Comparison of predicted and measured values.

3.3.1. Grey Correlation Analysis Method. Grey relational analysis method can analyse and compare various factors with different dimensions, and study the influence degree of each factor. The specific calculation steps are as follows.

(1) Establish a grey matrix X and Y

The comparison matrix X composed by the data of various influencing factors and the reference matrix Y composed by the corresponding representative indexes are established as follows:

$$X = \begin{bmatrix} x_{11} & \cdots & x_{1n} \\ \vdots & & \vdots \\ x_{m1} & \cdots & x_{mn} \end{bmatrix}, \quad (1)$$

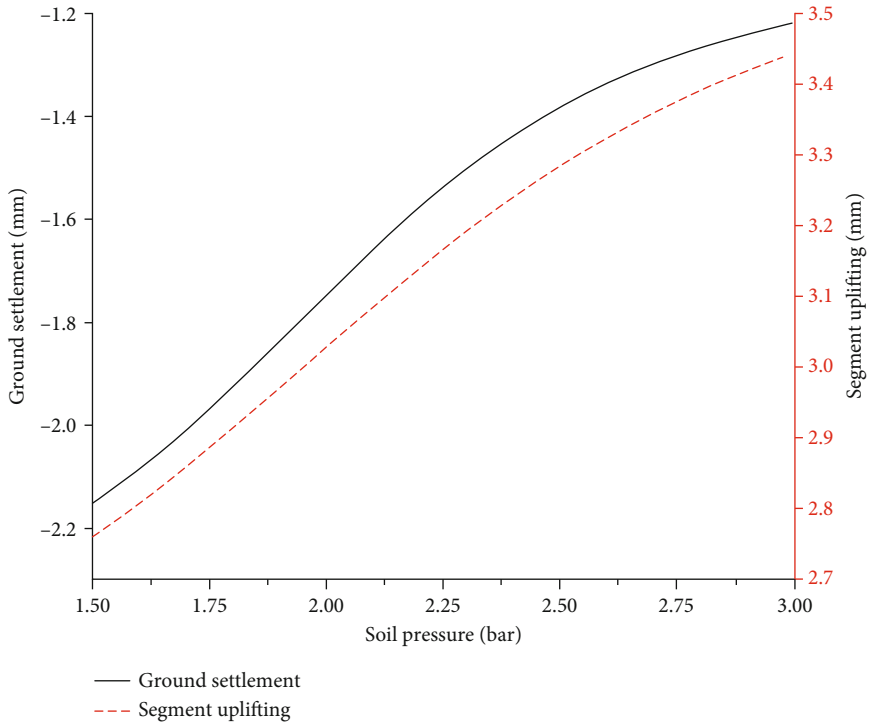

(a) Impact of soil pressure

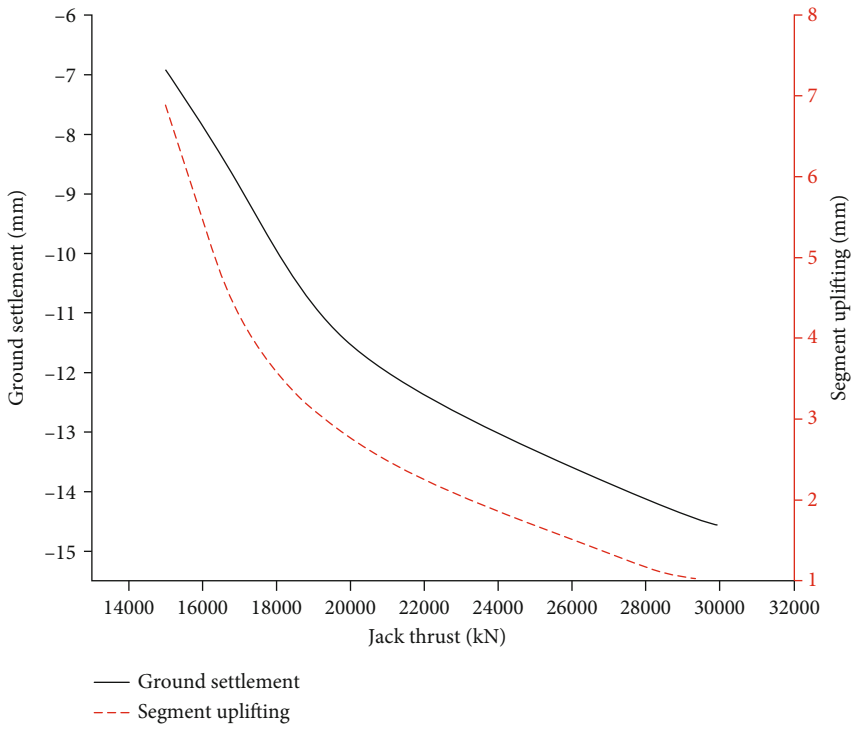

(b) Impact of jack thrust

Figure 7: Continued.

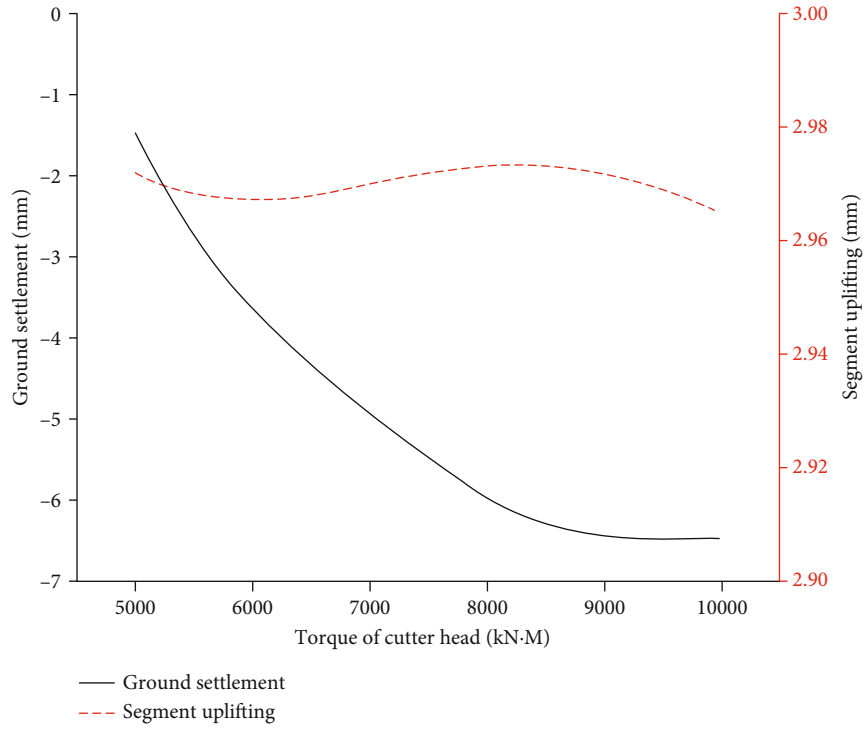

(c) Impact of cutter head torque

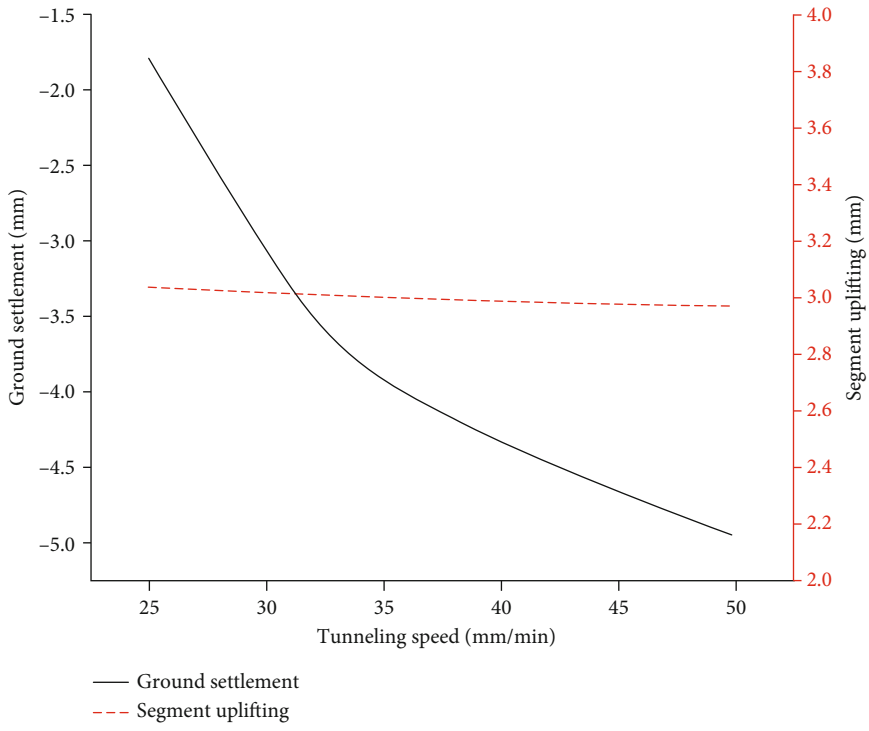

(d) Impact of tunneling speed

Figure 7: Continued.

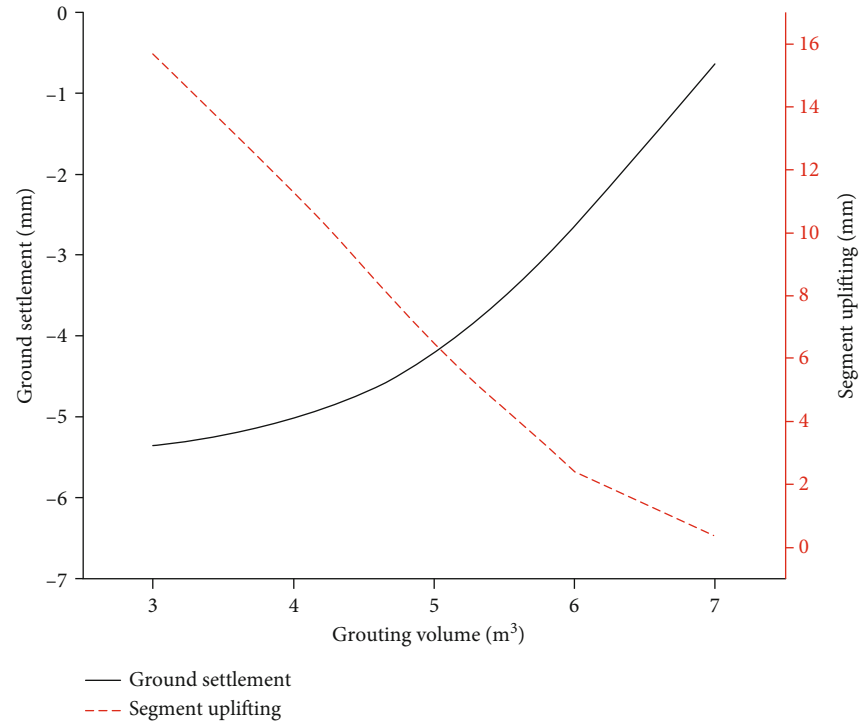

(e) Impact of grouting volume

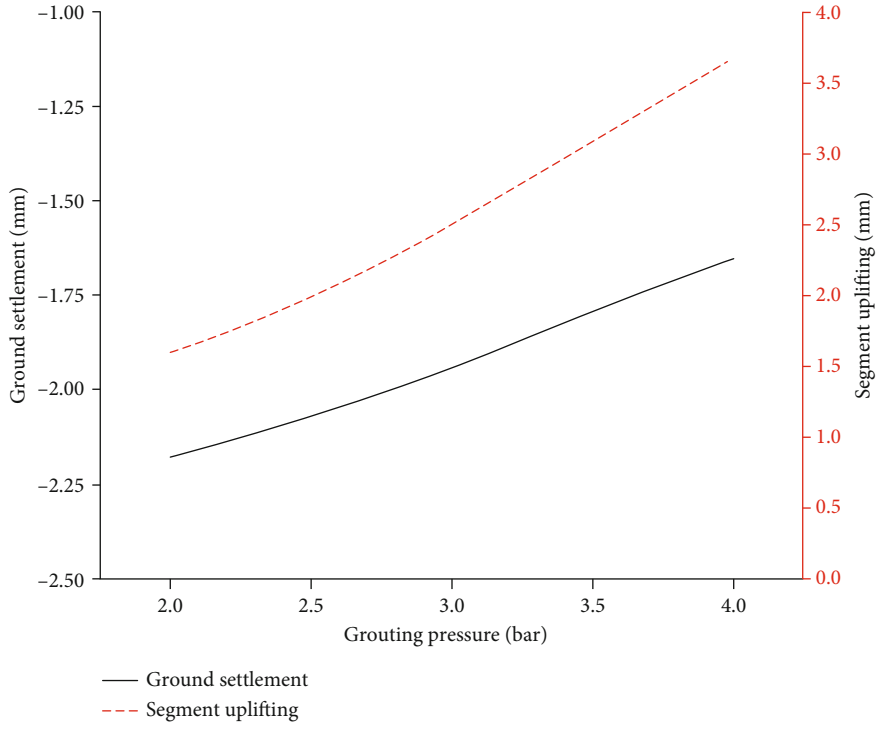

(f) Impact of grouting pressure

Figure 7: Continued.

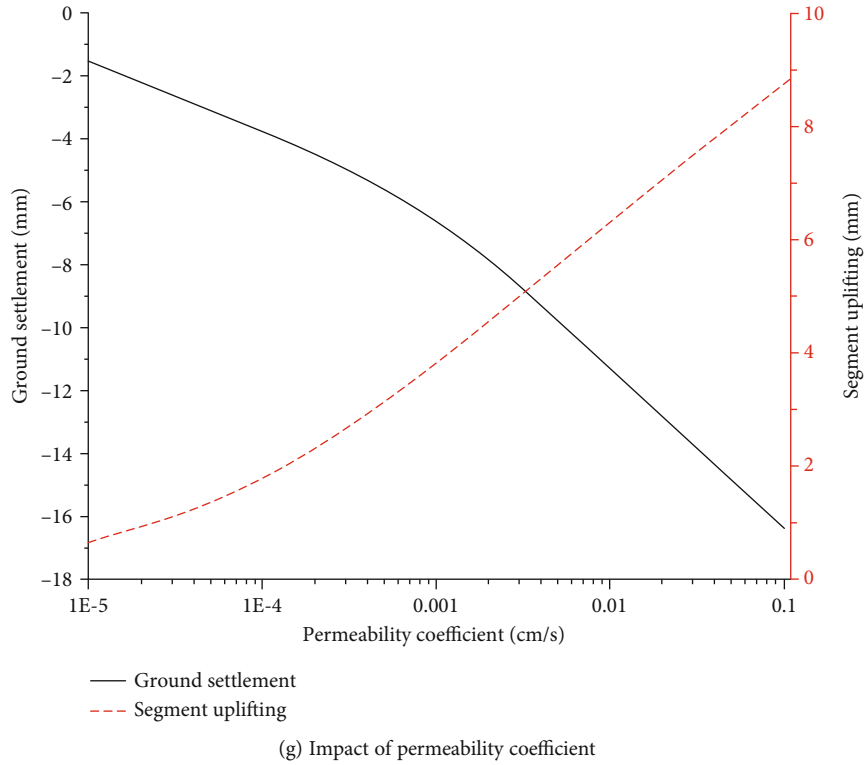

(g) Impact of permeability coefficient

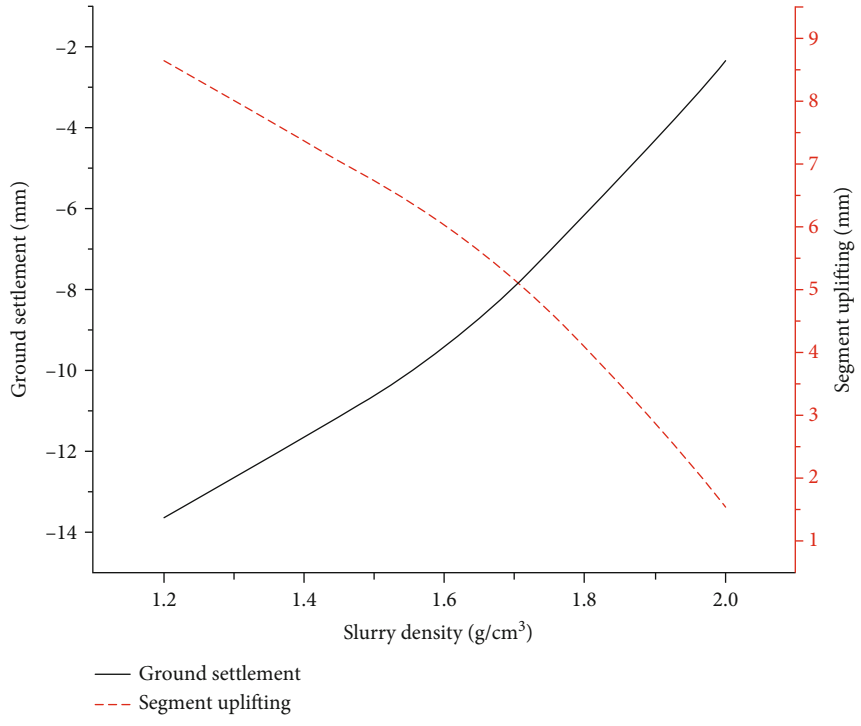

(h) Impact of slurry density

Figure 7: The variation curve of surface settlement and segment uplifting with construction parameters.

Table 4: Summary of influencing factors and corresponding settlement values.

Influence factors		Level of each factor (n)			
		1	2	3	4
Soil pressure	Pressure (bar)	1.5	2.0	2.5	3.0
	Settlement (mm)	2.15	1.75	1.38	1.22
Jack thrust	Thrust (kN)	16*e*3	20*e*3	24*e*3	28*e*3
	Settlement (mm)	7.81	11.54	13.01	14.12
Cutter head torque	Torque (kN·m)	5*e*3	6*e*3	8*e*3	10*e*3
	Settlement (mm)	-1.51	-3.68	-5.95	-6.47
Tunneling speed	Speed (mm/min)	25	30	35	45
	Settlement (mm)	-1.80	-3.01	-3.93	-4.65
Grouting volume	Volume (m^3)	3	4	5	6
	Settlement (mm)	-5.34	-5.11	-4.35	-2.57
Grouting pressure	Pressure (bar)	2.0	2.5	3.0	3.5
	Settlement (mm)	-2.18	-2.07	-1.95	-1.79
Permeability coefficient	Coefficient (cm/s)	1e-4	1e-3	0.01	0.1
	Settlement (mm)	3.68	6.23	11.24	16.37
Slurry density	Density (g/cm^3)	1.2	1.4	1.6	1.8
	Settlement (mm)	13.65	11.64	9.63	6.23

$$Y = \begin{bmatrix} y_{11} & \cdots & y_{1n} \\ \vdots & & \vdots \\ y_{m1} & \cdots & y_{mn} \end{bmatrix}, \quad (2)$$

where m is the number of influencing factors, and here, it is 8. n is the level of each factor, and it is 4.

(2) Dimensionless method

The dimensionless of the above matrix is as follows.

$$X_i' = \left[x_{i1}' \cdots x_{in}'\right], Y_i' = \left[y_{i1}' \cdots y_{in}'\right], i = 1, \cdots, m, \quad (3)$$

where

$$x_{ij}' = \frac{x_{ij} - \min x_{ij}}{\max x_{ij} - \min x_{ij}}, \quad (4)$$

$$y_{ij}' = \frac{y_{ij} - \min y_{ij}}{\max y_{ij} - \min y_{ij}}, \quad (5)$$

where $i = 1, \cdots, m$; $j = 1, \cdots, n$.

(3) Calculating the correlation coefficient

$$\xi_{ij} = \frac{\Delta(\min) + \rho\Delta(\max)}{\Delta_{ij} + \rho\Delta(\max)}, \quad (6)$$

where

$$\Delta(\min) = \min \left|y_{ij}' - x_{ij}'\right|, \quad (7)$$

$$\Delta(\max) = \max \left|y_{ij}' - x_{ij}'\right|, \quad (8)$$

$$\Delta_{ij} = \left|y_{ij}' - x_{ij}'\right|, \quad i = 1, \cdots, m, j = 1, \cdots, n. \quad (9)$$

ρ is the coefficient of resolution which usually takes as 0.5.

(4) Calculating correlation degree

The correlation degree of influencing factor is calculated as follows:

$$\gamma_i = \frac{1}{n}\sum_{j=1}^{n} \xi_{ij}. \quad (10)$$

Comparing the correlation degree of each influencing factor, the larger the value is, the more sensitive the ground settlement to this factor will be, and the more attention should be paid to this factor in the future study.

3.3.2. Calculation and Analysis. Due to the reasonable uplifting value of the segments, the focus of this section is on the sensitive analysis of ground settlement. The representative parameters of each influencing factors and the corresponding representative indexes are summarised, as shown in Table 4. The grey matrices X and Y can be computed according to Equations (1) and (2) are as follows.

Table 5: Summary of sensitivity coefficient.

Influence factors	Correlation coefficient
Soil pressure	0.4625
Jack thrust	0.8550
Cutter head torque	0.8250
Tunneling speed	0.8550
Grouting volume	0.5200
Grouting pressure	0.4725
Permeability coefficient	0.8450
Slurry density	0.4825

Table 6: Summary of construction parameters.

Influence factors	Section/rings	
	0~50	50~150
Soil pressure (bar)	1~1.3	1.3
Jack thrust (kN)	12000~18000	16000~24000
Cutter head torque (kN·m)	5000~6000	7500~8500
Tunneling speed (mm/min)	20~30	25~35
Grouting volume (m^3)	4.5~6.0	4.5~6.0
Grouting pressure (bar)	2~3	3~4
Permeability coefficient (cm·s)	$2.66e-2$	$2.66e-2$
Slurry density (g/cm^3)	1.32	1.32

$$X = \begin{bmatrix} 1.5 & 2.0 & 2.5 & 3.0 \\ 16e3 & 20e3 & 24e3 & 28e3 \\ 5e3 & 6e3 & 8e3 & 10e3 \\ 25 & 30 & 35 & 45 \\ 3 & 4 & 5 & 6 \\ 2.0 & 2.5 & 3.0 & 3.5 \\ 1e-4 & 1e-3 & 0.01 & 0.1 \\ 1.2 & 1.4 & 1.6 & 1.8 \end{bmatrix}, \quad (11)$$

$$Y = \begin{bmatrix} 2.15 & 1.75 & 1.38 & 1.22 \\ 7.81 & 11.54 & 13.01 & 14.12 \\ 1.51 & 3.68 & 5.95 & 6.47 \\ 1.8 & 3.01 & 3.93 & 4.65 \\ 5.34 & 5.11 & 4.35 & 2.57 \\ 2.18 & 2.07 & 1.95 & 1.79 \\ 3.68 & 6.23 & 11.24 & 16.37 \\ 13.65 & 11.64 & 9.63 & 6.23 \end{bmatrix}, \quad (12)$$

where $X$is the influencing factors, $Y$is the corresponding ground settlement under different influencing factors.

Using Equation (3), the dimensionless results are as follows.

$$X' = \begin{bmatrix} 0 & 0.33 & 0.66 & 1 \\ 0 & 0.33 & 0.66 & 1 \\ 0 & 0.2 & 0.6 & 1 \\ 0 & 0.25 & 0.5 & 1 \\ 0 & 0.33 & 0.66 & 1 \\ 0 & 0.33 & 0.66 & 1 \\ 0 & 9e\text{-}3 & 0.099 & 1 \\ 0 & 0.33 & 0.66 & 1 \end{bmatrix}, \quad (13)$$

$$Y' = \begin{bmatrix} 1 & 0.57 & 0.17 & 0 \\ 0 & 0.59 & 0.82 & 1 \\ 0 & 0.44 & 0.90 & 1 \\ 0 & 0.42 & 0.75 & 1 \\ 1 & 0.92 & 0.64 & 0 \\ 1 & 0.72 & 0.41 & 0 \\ 0 & 0.20 & 0.60 & 1 \\ 1 & 0.73 & 0.46 & 0 \end{bmatrix}. \quad (14)$$

Based on Equation (6), the corresponding correlation coefficient is as follows.

$$\xi_{ij} = \begin{bmatrix} 0.33 & 0.69 & 0.5 & 0.33 \\ 1 & 0.66 & 0.76 & 1 \\ 1 & 0.68 & 0.62 & 1 \\ 1 & 0.75 & 0.67 & 1 \\ 0.33 & 0.46 & 0.96 & 0.33 \\ 0.33 & 0.56 & 0.67 & 0.33 \\ 1 & 0.72 & 0.66 & 1 \\ 0.33 & 0.56 & 0.71 & 0.33 \end{bmatrix}. \quad (15)$$

Finally, the values of a correlation degree corresponding to the eight factors can be obtained, as summarised in Table 5. It can be seen from Table 5 that jack thrust, cutter head torque, tunneling speed, and permeability coefficient are the main factors affecting surface settlement, and their correlation coefficients are 0.855, 0.825, 0.855, and 0.845, respectively. In addition, the soil pressure, grouting volume, grouting pressure, and grout density are secondary influencing factors, and their correlation coefficients are 0.463, 0.520, 0.473, and 0.483, respectively.

3.3.3. Determination of Improvement Objects. Through the analysis of the correlation degree of the influencing factors in the previous section, this section will analyse the actual

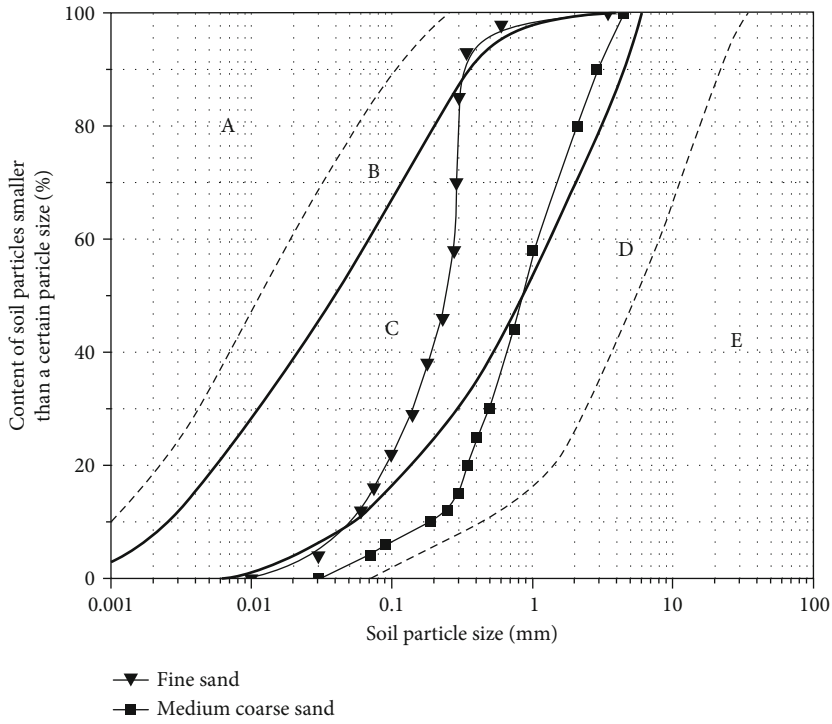

Figure 8: Gradation map of the layer. (A) Shield is not applicable. (B) Clay improvement. (C) No or little soil improvement. (D) Coarse grained soil improvement. (E) Shield is not applicable.

Table 7: Parameters of sandy soil layers.

Soil layer number	Soil layer name	Effective particle size d_{10} (mm)	Intermediate particle size d_{30} (mm)	The average particle size d_{50} (mm)	Boundary particle size d_{60} (mm)	Coefficient of unevenness (Cu)	Curvature coefficient (Cc)	Natural dip (°)	
								Overwater	Underwater
2-3	Fine sand	0.052	0.105	0.221	0.232	4.46	0.91	29.63	26
2-4	Coarse sand	0.173	0.418	0.712	1.113	6.43	0.90	29.94	28.33
7-2	Coarse sand	0.292	0.801	2.584	4.656	16.162	0.53	—	—

construction parameters one by one to determine the parameters that need to be improved. The construction parameters of shield tunneling are shown in Table 6. From Table 6 and Figure 7, it can be found that both jack thrust and tunneling speed all be controlled within a reasonable range, and the settlement value generated is within 5 mm. However, the cutter head torque and permeability coefficient are larger, and it can be seen from Figure 6 that they will produce a large settlement. Among them, the settlement caused by the excessive permeability coefficient exceeds 10 mm. Therefore, among the main influencing factors, the permeability coefficient of layer and the cutter head torque must be improved.

At the same time, through the analysis of the secondary influencing factors, it can be found that the soil pressure, grouting volume, grouting pressure, and slurry density are all controlled within a reasonable range (<5 mm), which have little influence on the settlement. Therefore, the next work is to improve the permeability of the excavated layer and reduce the cutter head torque appropriately to control the surface settlement.

4. Methods to Improve Ground Settlement

4.1. Stratigraphic Analysis. The permeability coefficient is related to the soil particle gradation of the layer, and the cutter head torque depends on the difficulty of excavation. It can be seen from the analysis results of geological conditions (Section 2) and Figure 2 that the shield tunnel passes through the full-sand layer. According to the particle size distribution curve of the soil layer which the shield tunnelled through (Figure 8), the two-layer gradation is uneven. In Figure 8, area C is the most suitable soil layer for soil pressure balance shield, and the soil can basically meet the requirements of plastic flow. In area B, there are a large number of fine particles, and the soil in this area is likely to adhere to the shield cutter head, resulting in the cutter

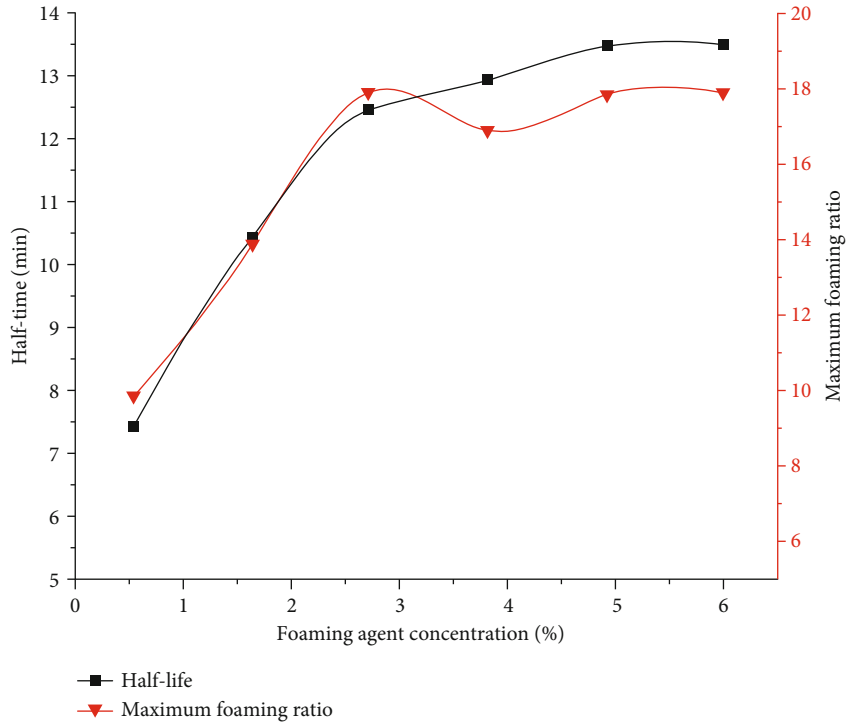

Figure 9: Foam optimisation experiment results.

head torque to be too large. Similarly, area A is sand with a finer particle diameter, which is less suitable for shield construction. Area D is a region with a large content of coarse particles, in which there are large gaps between the soil particles and the water permeability is strong. When the soil particles increase further to the coarse gravel sand layer (area E), the soil pressure balance shield is no longer applicable [24, 25]. Besides, from Table 7, the coefficients of unevenness for fine sand are Cu = 4.46 and Cc = 0.91, and the coefficients of unevenness for medium-coarse sand are Cu = 6.43 and Cc = 0.9. It can be found that these two layers are with low gradation according to the criterion of good gradation (Cu > 5, Cc = 1 ~ 3) in Standard for Engineering Classification of Soil for China [26]. The particles of the fine sand layer are too uniform, while the lack of certain coarse particles will cause the fine sand to adhere to the cutter head and increase the cutter head torque. Medium-coarse sand layers are mainly lacking particles in the interval of 0.1~0.25 mm and less than 0.05 mm, and the lack of fine particles makes the soil layer more permeable. Moreover, the sand layer is rich in water and has a micropressure type. When the shield is shut down for too long, a large amount of water in the pores of the layer may enter in the pressure chamber due to the greater permeability, leading to the "gushing" of the screw dumper outlet and resulting in excessive ground settlement or even collapse.

Therefore, it is necessary to improve the gradation and properties of the sandy soil layer to reduce the layer permeability coefficient and shear strength, that is, muck improvement.

4.2. Selection and Optimisation of Improvers

4.2.1. Selection of Improvers. In the improvement of shield mucks, the frequently used improvers are a foaming agent and sodium-based bentonite. Based on previous research, foaming agents can increase the fluidity of the soil and reduce the permeability coefficient. In the fine sand and clay layer, the existence of air bubbles prevents the muck from adhering to the cutter head panel and the pressure bulkhead, which is also helpful to reduce the cutter head torque [27, 28]. The volume expansion of the bentonite particles is 10 to 40 times of the original volume after absorbing water, which can form an impervious impermeable layer after absorbing water. Thus, the permeability coefficient can be reduced to less than 1×10^{-7} m/s [27, 28]. Therefore, bentonite is suitable for soils with low content of fine particles. The main reason is that bentonite mud can supplement the relatively small content of fine particles in coarse-grained soil for improving its water-stopping ability.

Due to the lack of 0.1-0.25 mm particles, there are too many soil particle voids in the medium-coarse sand layer, and the permeability coefficient reaches the order of 10^{-2} cm/s (Table 2). Therefore, it is difficult to effectively fill the particle voids by adding foam alone. In this study, the medium-coarse sand layer will be improved by using a foaming agent combined with a certain amount of bentonite mud, and the fine sand layer is only improved by the foaming agent.

4.2.2. Improver Optimisation. Before improvement, the concentration and blending ratio of the improvers needs to be

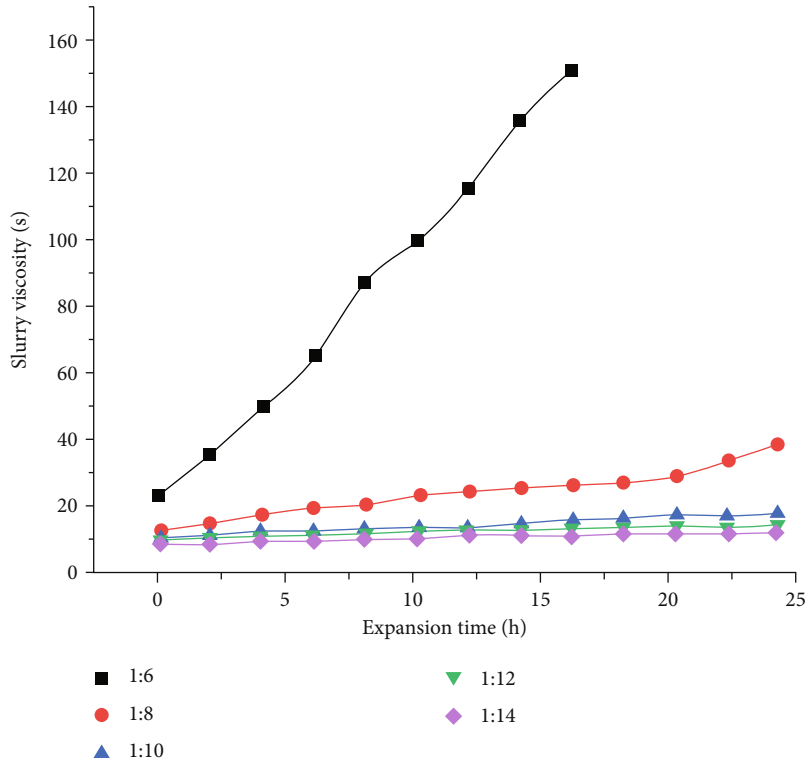

Figure 10: Relationship between the viscosity of sodium-based bentonite mud with puffing time.

determined. The foaming agent is MJSD-005, and the bentonite is Heishan Wancheng high-quality sodium-based bentonite, which specification is 200 mesh. The performance of the foam is mainly measured by its half-life and expansion ratio. The half-life of the foam is greater than 5 min, and the expansion ratio is 10-40, which can meet the requirements of earth pressure balance shield construction [29]. Bentonite mud is used to increase the fine particle composition in the soil layer, improve the plasticity of the soil layer, and reduce the friction between the soil particles. When the content of fine particle components (soil particle size < 0.07 mm) in the soil layer is less than 20%, mud is added. The mud test evaluates mud performance by measuring its funnel viscosity, which is appropriate between 30~40 s.

(1) Foam Concentration Optimisation. The relationship between the foaming agent concentration and performance when the design concentration is 1%, 2%, 3%, 4%, 5%, and 6% is shown in Figure 9.

From Figure 9, it can be seen that as the foaming agent concentration increases from 1% to 6%, the half-life of the foam increases from 7.5 min to 13.5 min. As the foaming agent concentration increases, the bubble is more stable. Moreover, as the foaming agent concentration increases from 1% to 3%, the half-life of the foam is from 7.5 min to 12.5 min, and in this range, the stability of the foam changes significantly. As the foaming agent concentration increases from 3% to 6%, the half-life of the foam increases from 12.5 min to 13.5 min, and in this range, the foam stability does not change seriously. From Figure 9, it can also be seen that the maximum expansion ratio of the foaming agent increases with the increase of the concentration of the foaming agent. When the concentration increases from 1% to 3%, the maximum expansion ratio improves from 10 to 18 times. When the concentration increases from 3% to 6%, the maximum expansion ratio is stable at about 18 times, and in this range, the expansion ratio is almost no longer affected by the concentration of the foaming agent. Therefore, the optimal foam concentration after foaming agent dilution is about 3%.

(2) Bentonite Mud Optimisation. As shown in Figure 10, when the bentonite mud concentration is less than 1 : 8 (the mud is thinner), the viscosity of the mud does not change significantly with the puffing time, and the final viscosity is less than 30 s. When the bentonite mud concentration is 1 : 6, the mud viscosity increased significantly with time, as the puffing time is 2 hours, and the viscosity of the mud reached 43.14 s. If it is entirely puffed, the time will be longer, and the viscosity of the mud will be too large, which will quickly lead to plugging. When the bentonite mud concentration is 1 : 8, it can reach the construction requirements after ten hours of expansion, and the viscosity at this time is 32.45 s. Therefore, from the perspective of expected effect and engineering cost, it is decided to use the bentonite mud of a concentration of 1 : 8, and the puffing time is 10 hours.

4.3. Muck Improvement

4.3.1. Prepare Soil Samples. Because the soil samples of the unexcavated section cannot be obtained easily, in order to

(a) $d > 5$ mm (b) 2 mm $< d <$ 5 mm

(c) 1 mm $< d <$ 2 mm (d) 0.5 mm $< d <$ 1 mm

(e) 0.25 mm $< d <$ 0.5 mm (f) 0.075 mm $< d <$ 0.25 mm

Figure 11: Screened soil with different particle sizes.

Figure 12: Prepared silty fine sand and medium-coarse sand.

make the test more reliable, this study will prepare the soil samples of the unexcavated section according to the geological survey report. Firstly, the soil (excavated muck) taken from the excavated section is dried and sieved. Then, the soil particles of each particle group are placed separately (Figure 11). Finally, according to the geological survey report, the dry sand is prepared (Figure 12). After the preparation of the dry sand, the saturated sand samples are prepared according to the saturated water content of the layer. According to the geological survey report, the saturated water content of the fine sand is 16% and the saturated water content of the medium and coarse sand is 11%. Then, the water and the prepared dry sand samples have been mixed, and the soil samples of the stratum can be obtained.

4.3.2. Seepage Test

(1) Test Mechanism. The penetration test is shown in Figure 13. The following equation can calculate the permeability coefficient K.

$$K = \frac{VL}{hAt}(\text{mm/s}), \tag{16}$$

where L is the height of soil, h is the head height, t is the drainage time (1 min), V is the drainage volume, and A is the instrument cross-sectional area.

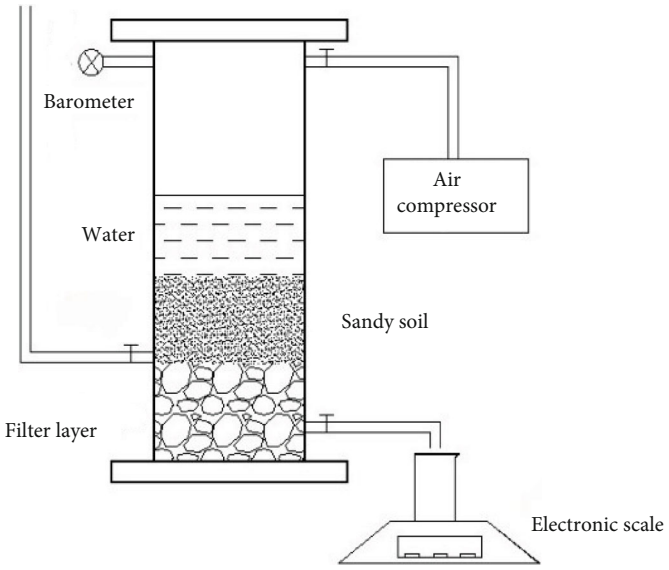

(a) Schematic diagram

(b) Real devices

Figure 13: Penetration test.

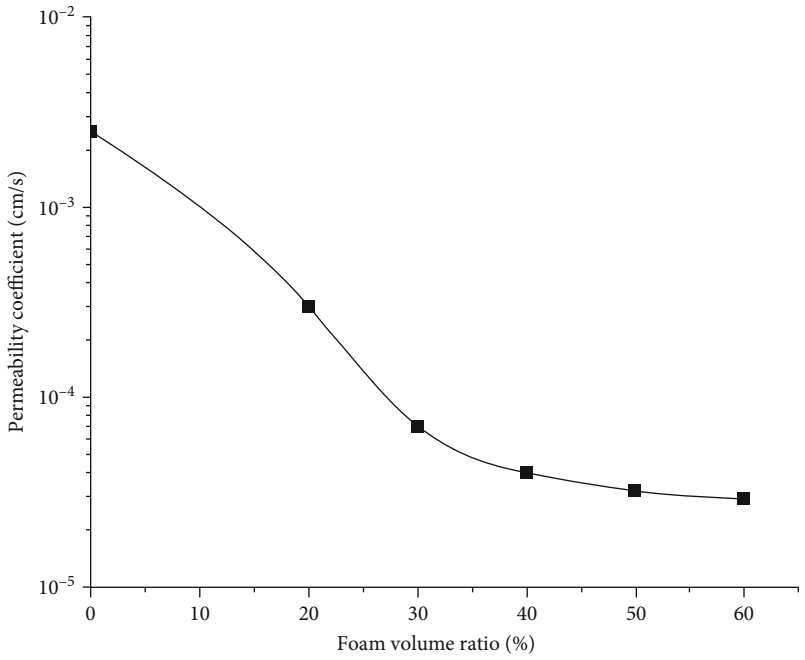

Figure 14: Relationship between foam content and permeability coefficient for fine sand.

Generally, when the permeability coefficient is less than 1×10^{-3} cm/s, which satisfies the requirement of "plastic flow" for soil body with permeability less than 10^{-3} cm/s under ideal conditions, the problem of "gushing" in the shield can be effectively avoided. The relationship between the pressure head and the water flow Q at the exit of the spiral ejector can be described as follows [30].

$$H_2 = H_1 - \frac{QL_1}{KA_1} - \frac{QL_2}{KA_2}, \tag{17}$$

where H_1 and H_2 are the heights of water pressure head on excavation side and on the spiral ejector outlet side, L_1 and L_2 are the pressure chamber length and ejector length, and A_1 and A_2 are the cross-sectional area of the pressure chamber and spiral ejector.

The mechanical parameters of the shield machine are as follows. L_1 and L_2 are 1.125 m and 10.039 m. D_1 and D_2 are 6 m and 0.77 m. In addition, H_1 is about 10 m. When the critical seepage flow at the outlet of the ejector is 3 cm^3/s, and the critical water pressure is 1 m, the permeability coefficient of

(a) (b) (c)

Figure 15: Improved fine sand with foam.

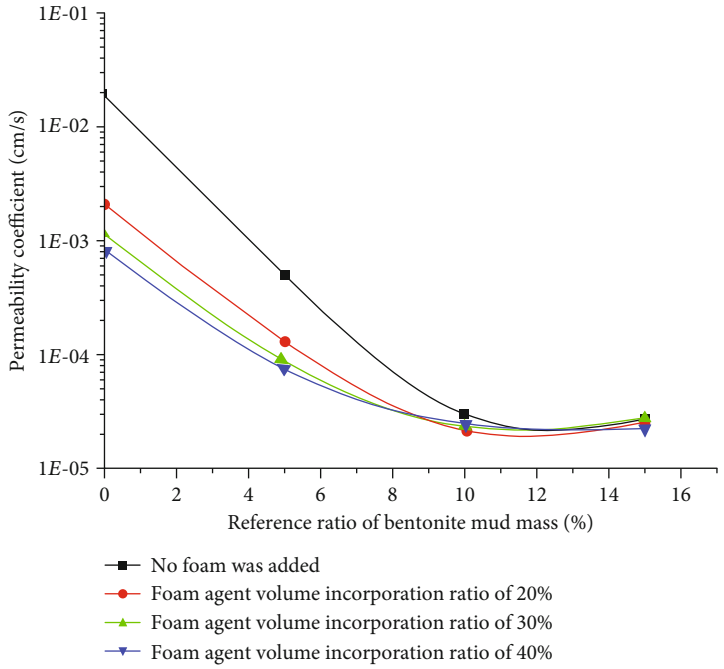

Figure 16: Permeability of medium-coarse sand mixed with foam and bentonite mud.

the soil when "gushing" occurs can be obtained as 7.21×10^{-3} cm/s based on Equation (17). Therefore, in order to prevent "gushing" during shield construction, the permeability coefficient of the improved soil must be less than this value.

(2) Result of Fine Sand. The relationship between the foaming agent blending ratio and the fine sand permeability coefficient is shown in Figure 14. From Figure 14, the permeability coefficient of the fine sand is 2.43×10^{-3} cm/s without improvement. As the amount of foaming agent increases, the permeability of sandy soil is significantly reduced. When the foam blending ratio is 40%, the permeability of the improved muck has been reduced to 3×10^{-5} cm/s. When the blending ratio of the foaming agent exceeds 40%, the decrease of muck permeability is not apparent. Figure 15 is the state of fine sand with different foam volume. From Figure 15, as too much foaming agent is added, the excess bubbles do not enter the soil, and the soil is mixed uniformly. These foams which did not reduce the water permeability will be discharged directly with water during the penetration test.

(3) Result of Medium-Coarse Sand. In this study, the combination of foaming agent and bentonite mud was used to improve the medium-coarse sand. As shown in Figure 16, the medium-coarse sand has a permeability coefficient of 2.02×10^{-2} cm/s without improvement. When the blending ratio of the foaming agent is 40%, and without adding bentonite, the permeability coefficient is 8.34×10^{-4} cm/s. When the blending ratio of bentonite mud is 10%-15% on the basis of 40% foaming agent, the permeability coefficient decreases to 2×10^{-5} cm/s, which can further reduce the risk of "gushing."

4.3.3. Direct Shear Test

(1) Test Mechanism. According to Coulomb's law, the internal friction of the soil is proportional to the normal pressure

Table 8: Results of direct shear test of fine sand.

Soil sample	Foam volume blending ratio (%)	Vertical pressure (kPa)	Micrometer reading (0.01 mm)	Shear strength (kPa)	Cohesion (kPa)	Internal friction angle (°)
Fine sand	0	50	17	28.76	3.5	26.8
		100	31.5	54.01		
		200	60.5	104.53		
		300	94	162		
	30	50	15	26.13	4.7	23.9
		100	27.5	47.56		
		200	52.5	90.42		
		300	77.5	133.28		
	40	50	13.5	23	2.9	21.9
		100	25	43.1		
		200	48.5	83.3		
		300	75	125.5		

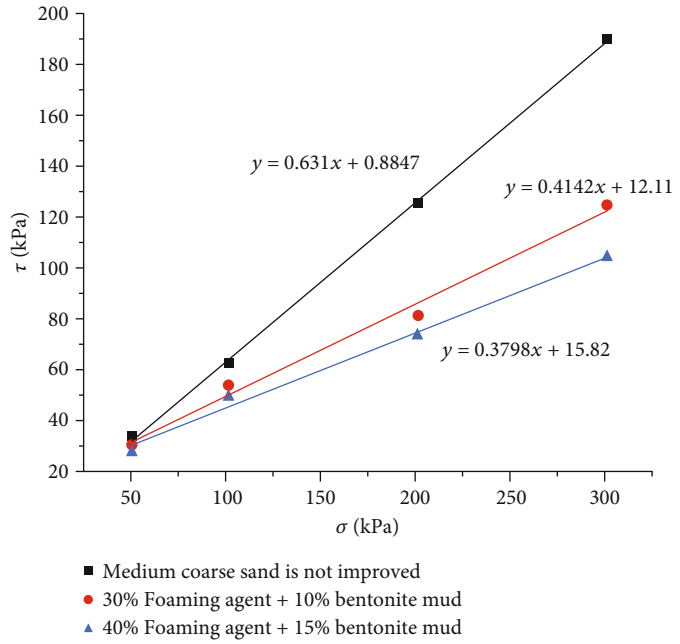

Figure 17: Shear strength of medium-coarse sand before and after improvement.

on the shear surface. Several soil samples are prepared from the same soil; their size is unified as 30 $cm^2 \times 2$ cm and then put the samples in the direct shear instrument. The horizontal shear force is directly applied along the fixed shear plane under different normal pressures (50 kPa, 100 kPa, 200 kPa, and 300 kPa), and the shear stress is the shear strength when the samples are damaged. And then, the internal friction angle ϕ and cohesion c for the soil can be determined according to the shear law.

(2) Results of Fine Sand. The experimental results are shown in Table 8. As can be seen from Table 8, the shear strength of the fine sand sample is 162 kPa under a vertical pressure of 300 kPa; the shield cutter head needs to overcome larger torque. When the foam blending ratio increases, the internal friction angle is significantly reduced. The internal friction angle of fine sand is reduced from 26.8° to 21.9° with the foam blending ratio increases from 0 to 40%. Furthermore, the shear strength is reduced to about 125 kPa, which can effectively reduce the wear on the cutter head and the cutter head torque.

(3) Results of Medium-Coarse Sand. From Figure 17, the shear strength of the unimproved medium-coarse sand under the vertical pressure of 300 kPa is 192.55 kPa, which may cause excessive torque of the shield cutter head. When the blending ratio of foam is 30%, and the blending ratio of bentonite mud is 10%-15%, the internal friction angle of the medium-coarse sand decreases from 32.3° to about 22.5°, and the shear strength under 300 kPa pressure

(a) Unimproved

(b) 30%foam + 5%bentonite

(c) 30%foam + 10%bentonite

(d) 30%foam + 15%bentonite

(e) 40%foam + 10%bentonite

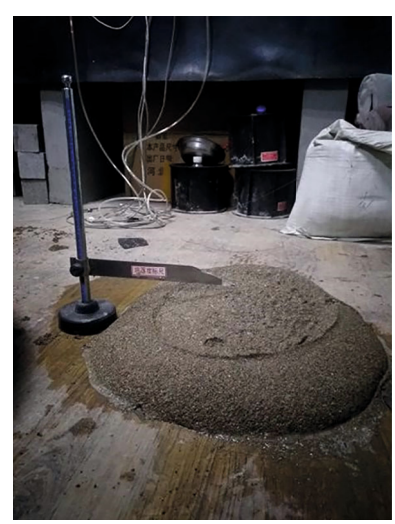

(f) 40%foam + 15%bentonite

Figure 18: Slump test of medium-coarse sand.

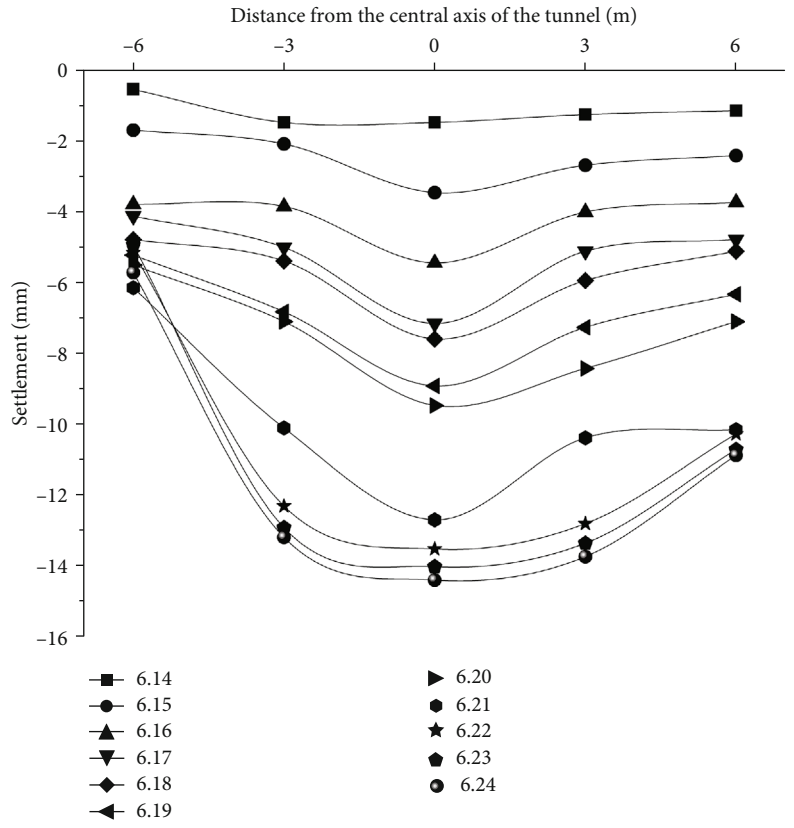

(a) Settlement monitoring of 238th ring

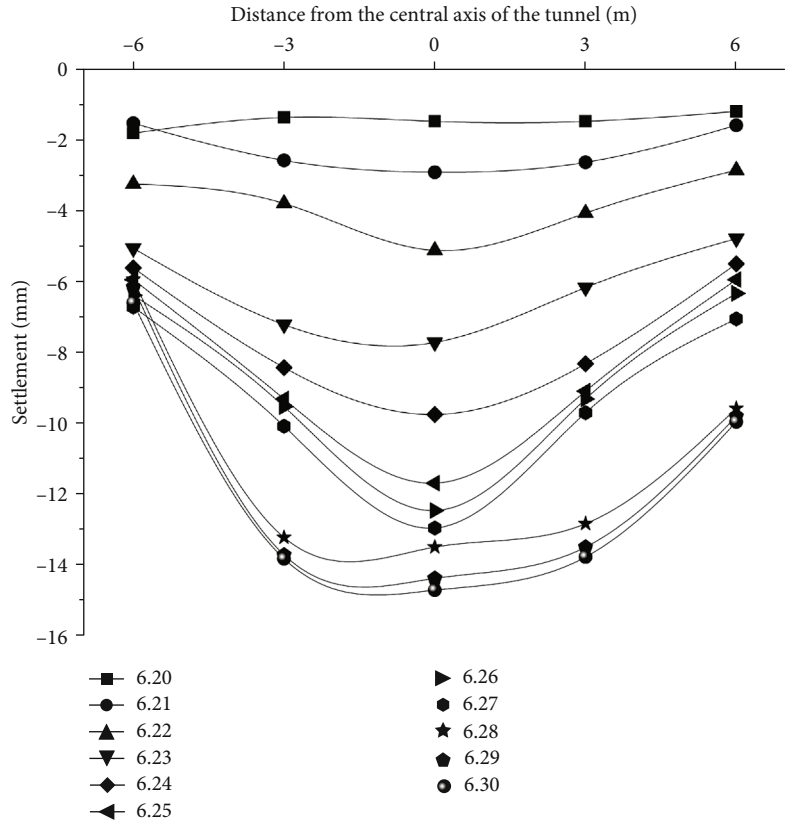

(b) Settlement monitoring of 287th ring

Figure 19: Continued.

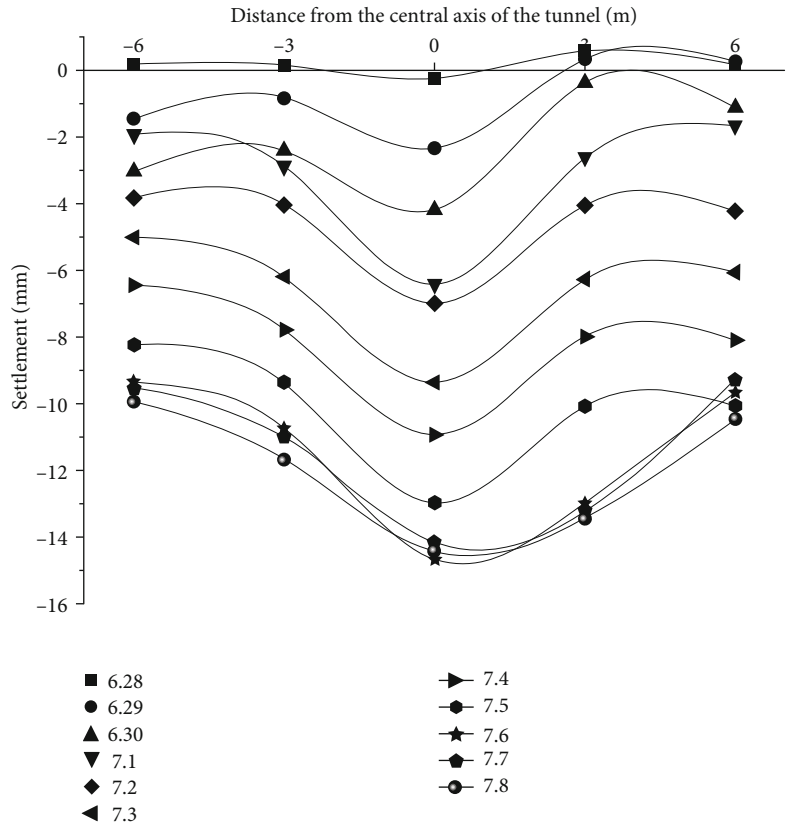

(c) Settlement monitoring of 378th ring

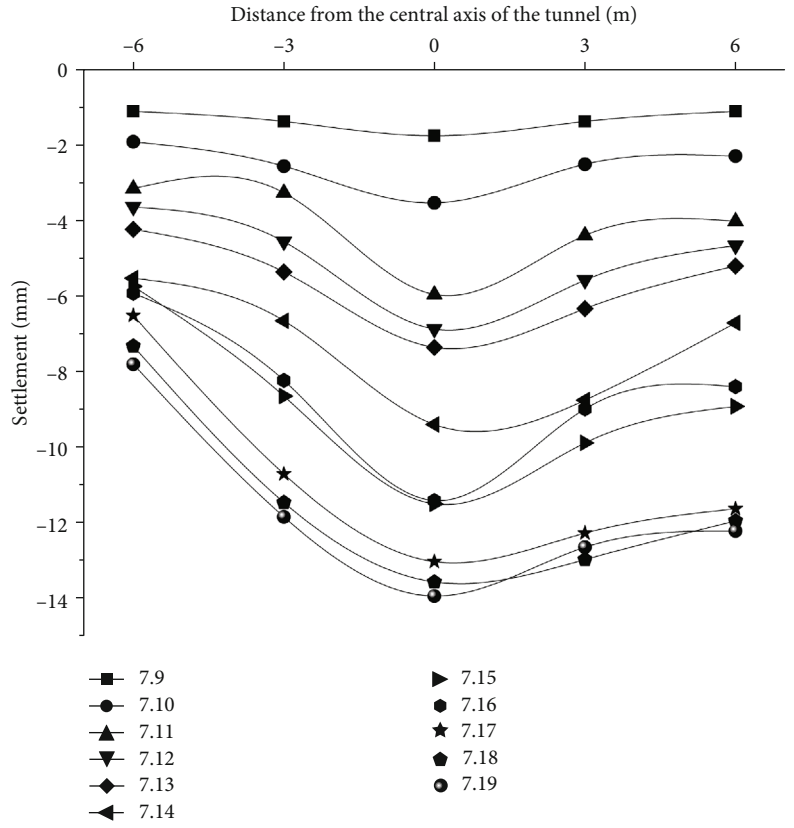

(d) Settlement monitoring of 436th ring

Figure 19: Surface settlement of different sections after 150 rings.

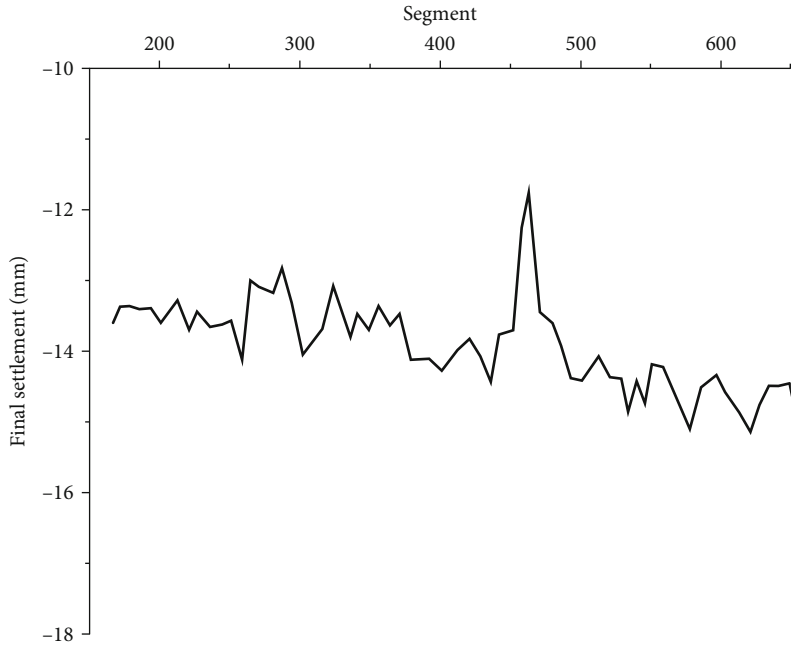

Figure 20: Final surface settlement of the right line after 150th ring.

decreases to 105 kPa-125 kPa, which can effectively reduce the wear on the cutter head and reduce the cutter head torque. When the foam blending ratio is increased to 40%, the improvement effect of the shear strength is better. However, learning from the improvement of fine sand, it is not that more bubbles mean better.

At the same time, the optimal blending ratio of foam and bentonite is analysed by the slump test (Figure 18). The sludge measured for the medium-coarse sand samples is only 20 mm, and there is almost no slump. Then, the fluidity of the soil sample is very poor. When the blending ratio of the foaming agent is 30% and the blending ratio of bentonite mud is from 5% to 15%, the slump is between 155 mm and 195 mm. When the foam blending ratio is 40%, the slump exceeds 200 mm. At this time, the plasticity of soil is low, and a large amount of water and foam are precipitated. Then, the improvement effect becomes poor. In addition, the effect of improving permeability is similar when the foam content is 30% and 40%. Therefore, it is more appropriate to use a foam volume blending ratio of 30% and a mass blending ratio of 10% to 15% for bentonite mud to improve the medium-coarse sand. The permeability coefficient of medium-coarse sand at this time is $2.47 \times 10^{-5} - 3.69 \times 10^{-5}$ cm/s, and the shear strength under 300 kPa pressure is 105-125 kPa.

4.3.4. Application of Improvers. According to the above test analysis, the shear strength and permeability coefficient of saturated fine sand can be reduced by adding foam with a blending ratio of 40%. Among them, the magnitude of the permeability coefficient is reduced from 10^{-3} to 10^{-5}, and the shear strength is reduced by 22.84%. For medium-coarse sand layer, it is appropriate to use a foam volume blending ratio of 30%, and a mass blending ratio of 10% to 15% of bentonite mud, the magnitude of the permeability coefficient is reduced from 10^{-2} to 10^{-5}, and the shear strength is reduced by 35.08%-45.46%. They can effectively reduce the permeability coefficient of the layer and indirectly reduce the cutter torque.

After the proportion of improver is determined, the on-site workers transport the mixed bentonite slurry and foam through the pipeline to the storage box of the shield machine, and inject it into the front of the cutter head and the soil bin in time. When the shield traverses mainly fine sand layer, each ring is injected with a volume of 40% foam mixture, and the original foam is 25 L; when the shield traverses mainly medium-coarse sand layer, 19 L original foam is used for each ring and injected bentonite mud simultaneously; the use of bentonite mud is about 7.5 m^3 per ring.

4.4. Effect of Muck Improvement. During the shield tunneling, to study the effect of muck improvement on the ground settlement, the settlement after the 150th ring has been monitored. At this time, the cutter head torque is adjusted to 4500-5500 kN according to the reduction in the shear strength of the muck (35%-45%), and other construction parameters remain unchanged. Several settlement fluctuations were selected to analyse the settlement before the shield machine arrived and after the synchronous grouting was completed. The ground settlement curves are as shown in Figure 19.

It can be seen from Figure 19 that the settlement curves of each section show settlement grooves, which are symmetrically distributed on the central axis. The settlement speed of the ground before the shield machine arrives relatively slow, and the settlement speed increases sharply as the shield machine passes. With the synchronous grouting behind the wall and the departure of the shield machine, the settlement gradually slows down and finally stabilises. The whole process lasts about ten days until it finally stabilises. The

improvement of muck can better control the ground settlement, and it is controlled within 15 mm, which effectively solves the problem of excessive ground settlement.

The construction of the right line was completed on August 20, 2018. After the ground settlement stabilised, the whole settlement at the centre axis of the right line was analysed. As shown in Figure 20, before the 150th ring where the muck was not improved, the ground settlement on the right line exceeded the alert value (-20 mm/+7 mm) 6 times and exceeded the control value (-30 mm/+10 mm) 4 times. The maximum settlement on the right line occurred at 51st ring with a settlement of -31.53 mm. After the muck improved, the minimum and maximum settlements are -9.36 mm and -15.21 mm, respectively. Thus, the maximum settlement is reduced by 16.32 mm, and the reduction ratio reaches 51.76%. After the 150th ring, the average ground settlement on the right line was -13.63 mm, which is successfully controlled within the alert value. It can be seen that after the muck improvement, the average settlement is reduced by 9.17 mm compared with the settlement before improvement (-22.80 mm), and the reduction ratio is 40.22%.

Therefore, aiming at the surface settlement caused by shield construction in the high-permeability area of Harbin, the proposed method of muck improvement guided by the Deep Belief Network (DBN) has achieved complete success.

5. Conclusions

In response to the problem of excessive ground subsidence in the second phase of the Harbin Subway Line 3, this paper constructs a ground settlement prediction model with various construction parameters as input variables based on the Deep Belief Network (DBN), which studies the influence of various parameters on the settlement. Under the guidance of the DBN algorithm, the method of parameter improvement for controlling ground subsidence has been studied, and the main conclusions obtained are as follows:

(i) In the construction of the Harbin Subway Line No. 3, the cutter head torque, tunneling speed, jack thrust, and the permeability coefficient of the layer are the main factors affecting surface settlement, while the soil pressure, grouting volume, grouting pressure, and grout density are a secondary factor

(ii) Through the analysis of various parameters of the DBN model and the corresponding calculation of sensitivity, it is found that the surface subsidence is mainly caused by the excessive cutter head torque and the large permeability of the layer

(iii) Through analysing the gradation of soil particles in the layer, it is found that the excessive permeability is caused by uneven soil particles, and the excessive torque of the cutter head is caused by the higher shear strength of the soil particles. By adding a suitable foaming agent and bentonite to the layer to improve the muck, it has successfully reduced the permeability coefficient and shear strength of the formation

(iv) The decrease in the permeability of the muck is beneficial to reduce the occurrence of "gushing," which reduced interference to the excavation surface. And the reduction of the shear strength of the sand in the formation is beneficial to the reduction of the cutter head torque. Through the improvement of the above two parameters, the ground subsidence was successfully controlled within the warning range

Data Availability

The test data used to support the findings of this study are included within the article. Readers can obtain data supporting the research results from the test data table in the paper.

Conflicts of Interest

The authors declare that there is no conflict of interest regarding the publication of this paper.

Acknowledgments

This work was supported by the Postgraduate Research & Practice Innovation Program of Jiangsu Province (grant number KYCX20_0439) and the Fundamental Research Funds for the Central Universities.

References

[1] M. Sharghi, H. Chakeri, and Y. Ozcelik, "Investigation into the effects of two component grout properties on surface settlements," *Tunnelling and Underground Space Technology*, vol. 63, pp. 205–216, 2017.

[2] X. Y. Xie, Y. B. Yang, and M. Ji, "Analysis of ground surface settlement induced by the construction of a large-diameter shield-driven tunnel in Shanghai, China," *Tunnelling and Underground Space Technology*, vol. 51, pp. 120–132, 2016.

[3] F. Eskandari, K. G. Goharrizi, and A. Hooti, "The impact of EPB pressure on surface settlement and face displacement in intersection of triple tunnels at Mashhad Metro," *Geomechanics and Engineering*, vol. 15, no. 2, pp. 769–774, 2018.

[4] K. Kim, J. Oh, H. Lee, D. Kim, and H. Choi, "Critical face pressure and backfill pressure in shield TBM tunnelling on soft ground," *Geomechanics and Engineering*, vol. 15, no. 3, pp. 823–831, 2018.

[5] K. Cui and W. Lin, "Muck problems in subway shield tunneling in sandy cobble stratum," *Polish Maritime Research*, vol. 23, no. s1, pp. 175–179, 2016.

[6] D. Peila, A. Picchio, and A. Chieregato, "Earth pressure balance tunnelling in rock masses: laboratory feasibility study of the conditioning process," *Tunnelling and Underground Space Technology*, vol. 35, pp. 55–66, 2013.

[7] P. Fritz, "Additives for slurry shields in highly permeable ground," *Rock Mechanics and Rock Engineering*, vol. 40, no. 1, pp. 81–95, 2007.

[8] S. Psomas, *A thesis submitted for the degree of Master of Science to the University of Oxford*, St. Hugues's College of Oxford University, Michaelmas (OK), 2001.

[9] Y. G. Zhang, J. Tang, Z. Y. He, J. Tan, and C. Li, "A novel displacement prediction method using gated recurrent unit

model with time series analysis in the Erdaohe landslide," *Natural Hazards*, 2020.

[10] Y. G. Zhang, J. Tang, R. P. Liao et al., "Application of an enhanced BP neural network model with water cycle algorithm on landslide prediction," *Stochastic Environmental Research and Risk Assessment*, 2020.

[11] Y. Zhang, Z. Zhang, S. Xue, R. Wang, and M. Xiao, "Stability analysis of a typical landslide mass in the Three Gorges Reservoir under varying reservoir water levels," *Environment and Earth Science*, vol. 79, no. 1, 2020.

[12] Z. Zhang, M. Huang, C. Zhang, K. Jiang, and Q. Bai, "Analytical prediction of tunneling-induced ground movements and liner deformation in saturated soils considering influences of shield air pressure," *Applied Mathematical Modelling*, vol. 78, pp. 749–772, 2020.

[13] B. Gong, Y. J. Jiang, and P. Yan, "Discrete element numerical simulation of mechanical properties of methane hydrate-bearing specimen considering deposit angles," *Journal of Natural Gas Science and Engineering*, vol. 76, p. 103182, 2020.

[14] Y. LeCun, Y. Bengio, and G. Hinton, "Deep learning," *Nature*, vol. 521, no. 7553, pp. 436–444, 2015.

[15] R. Boubou, F. Emeriault, and R. Kastner, "Artificial neural network application for the prediction of ground surface movements induced by shield tunnelling," *Canadian Geotechnical Journal*, vol. 47, no. 11, pp. 1214–1233, 2010.

[16] R. P. Chen, P. Zhang, X. Kang, Z. Q. Zhong, Y. Liu, and H. N. Wu, "Prediction of maximum surface settlement caused by earth pressure balance (EPB) shield tunneling with ANN methods," *Soils and Foundations*, vol. 59, no. 2, pp. 284–295, 2019.

[17] D. Bouayad and F. Emeriault, "Modeling the relationship between ground surface settlements induced by shield tunneling and the operational and geological parameters based on the hybrid PCA/ANFIS method," *Tunnelling and Underground Space Technology*, vol. 68, pp. 142–152, 2017.

[18] H. M. Lyu, S. L. Shen, and A. N. Zhou, "Risk assessment of mega-city infrastructures related to land subsidence using improved trapezoidal FAHP," *Science of The Total Environment*, vol. 717, p. 135310, 2020.

[19] G. E. Hinton, S. Osindero, and Y. W. Teh, "A fast learning algorithm for deep belief nets," *Neural Computation*, vol. 18, no. 7, pp. 1527–1554, 2006.

[20] B. Zhao and C. J. Wu, "Sound quality evaluation of electronic expansion valve using Gaussian restricted Boltzmann machines based DBN," *Applied Acoustics*, vol. 170, p. 107493, 2020.

[21] Y. N. Zhu, L. Chen, and H. Zhang, "Quantitative analysis of soil displacement induced by ground loss and shield machine mechanical effect in metro tunnel construction," *Applied Sciences*, vol. 9, no. 15, p. 3028, 2019.

[22] K. Liu, J. K. Wu, H. B. Liu, M. Sun, and Y. Wang, "Reliability analysis of thermal error model based on DBN and Monte Carlo method," *Mechanical Systems and Signal Processing*, vol. 146, p. 107020, 2021.

[23] D. Rajamani, A. Ziout, and E. Balasubramanian, "Prediction and analysis of surface roughness in selective inhibition sintered high-density polyethylene parts: a parametric approach using response surface methodology-grey relational analysis," *Advances in Applied Mechanics*, vol. 10, no. 12, 2018.

[24] C. Budach and M. Thewes, "Application ranges of EPB shields in coarse ground based on laboratory research," *Tunnelling and Underground Space Technology*, vol. 50, pp. 296–304, 2015.

[25] S. Jancsecz, R. Krause, and L. Langmaack, "Advantages of soil conditioning in shield tunneling: experiences of LRTS Izmir," *Proceedings of World Tunnel Congress on Challenges for the 21st Century*, , pp. 865–875, Balkema, Rotterdam, 1999.

[26] Ministry of Water Resources of the People's Republic of China, *Standard for Engineering Classification of Soil (GB/T 50145-2007)*, China Planning Press, Beijing, 2008.

[27] S. Huang, S. Y. Wang, and C. J. Xu, "Effect of grain gradation on the permeability characteristics of coarse-grained soil conditioned with foam for EPB shield tunneling," *KSCE Journal of Civil Engineering*, vol. 23, no. 11, pp. 4662–4674, 2019.

[28] Z. Q. Huang, C. Wang, and J. Y. Dong, "Conditioning experiment on sand and cobble soil for shield tunneling," *Tunnelling and Underground Space Technology*, vol. 87, pp. 187–194, 2019.

[29] R. Vinai, C. Oggeri, and D. Peila, "Soil conditioning of sand for EPB applications: a laboratory research," *Tunnelling and Underground Space Technology*, vol. 23, no. 3, pp. 308–317, 2008.

[30] W. Zhu, J. S. Qin, and K. L. Wei, "Research on the mechanism of the spewing in the EPB shield tunnelling," *Chinese Journal of Geotechnical Engineering-Chinese Edition*, vol. 26, no. 5, pp. 589–593, 2004.